Indirect measurement of field emission electron current from the main superconducting cavities of compact ERL at KEK

Hiroshi Matsumura[1,*], *Hajime* Nakamura[1], *Akihiro* Toyoda[1], *Ken-ichi* Hozumi[1], *Hiroshi* Sakai[1], *Kazuhiro* Enami[1], *Takaaki* Furuya[1], *Kenji* Shinoe[1], *Kensei* Umemori[1], *Kaiichi* Haga[1], *Shogo* Sakanaka[1], *Masaru* Sawamura[2], and *Enrico* Cenni[3]

[1]High Energy Accelerator Research Organization (KEK), Tsukuba, Ibaraki 305-0801, Japan
[2]Japan Atomic Energy Agency (JAEA), Tokai-mura, Ibaraki 319-1195, Japan
[3]The Graduate University for Advanced Studies, Tsukuba, Ibaraki 305-0801, Japan

Abstract. The field emission electron currents from the main superconducting cavities (Cavities #3 and #4) of compact ERL at KEK, Japan, were estimated indirectly from photon dose rates measured around the cavities and on the roof of the compact ERL room. The field emission electron currents estimated from the photon dose rates measured around the cavities are in good agreement with those on the roof of the compact ERL room. The field emission electron currents increased steeply with the applied voltage. The field emission electron currents corresponding to the applied voltages were different between Cavity #3 and Cavity #4. We found that the field emission electron current exceeded 1 μA at 13.5 MV for Cavity #3 and at 15.5 MV for Cavity #4. This result was used in considering unexpected loss of field emission electrons.

1 Introduction

The compact Energy Recovery Linac (compact ERL)—an electron accelerator with a maximum energy of 26 MeV—has been under development at the compact ERL room at KEK, Tsukuba, Japan [1]. The compact ERL consists partly of the injector and the recirculating loop, as shown in Figure 1. Electrons are accelerated to a maximum energy of 6 MeV in the injector. The accelerated electrons are transferred to the recirculating loop and accelerated to a maximum energy of 26 MeV by a set of main superconducting cavities (Cavities #3 and #4) [2]. The 26 MeV electrons are transported round the recirculating loop until they reach the main superconducting cavities again. Subsequently, the electrons are decelerated to 6 MeV in the main superconducting cavities, and finally, the beam is terminated at the beam dump. In the compact ERL, the main superconducting cavities play an important role for acceleration and deceleration of electrons.

When a voltage is applied to the main superconducting cavities, field emission electrons are generated inside those cavities [3]. A portion of the generated electrons is accelerated inside the cavities in the same way as operated electron beam and consequently emitted from both ends of the superconducting cavities. Loss of field emission electrons in the recirculating loop is considered an unexpected radiation source. Before the main superconducting cavities (Cavities #3 and #4) were

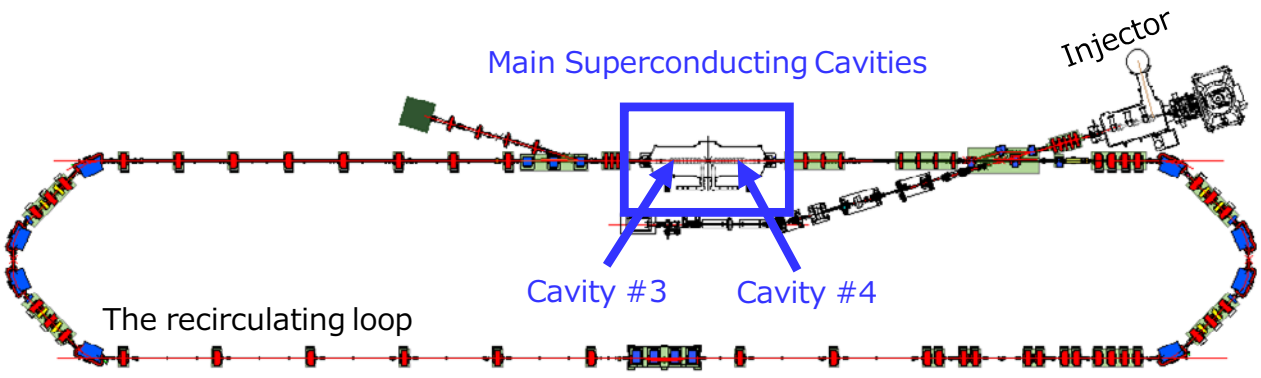

Fig. 1. Location of the main superconducting cavities in compact ERL installed in the compact ERL room in KEK. The main superconducting cavities consist of Cavities #3 and #4.

* Corresponding author: hiroshi.matsumura@kek.jp

installed in the compact ERL in 2014, we had to know whether the field emission electron current was acceptable for machine safety and radiation safety.

In this study, therefore, we indirectly measured the field emission electron current from each main superconducting cavity. In particular, the field emission electron currents were obtained through measurements and simulations of secondary radiation photons and subsequently compared. The secondary photons were produced by bombarding stainless steel (SUS) blind flanges, used for closing both ends of the superconducting cavities, with field emission electrons.

2 Measurements

2.1 Outline of measurements

During measurements of the field emission electron currents from the main superconducting cavities, the assembly of the main superconducting cavities were closed using 1-cm-thick SUS blind flanges. Furthermore, 20-cm-thick lead and 50-cm-thick concrete shield blocks were added to each side of the main superconducting cavities, as shown in Figures 2a and 2b.

While a voltage was applied to each main superconducting cavity, the field emission electrons are generated and accelerated inside their own cavity. The SUS blind flanges are bombarded with the accelerated electrons and bremsstrahlung was consequently generated. We can indirectly estimate the field emission electron current from the flux of the photons generated at the SUS blind flanges. In this study, the photon flux was measured as photon dose rate.

The field emission electrons can be accelerated toward both ends of a superconducting cavity. However, a previous study [3] found that the field emission electron currents in Cavities #3 and #4 were quite different in opposing directions. In the case of Cavity #4, the intensity of the electrons emitted to the right in Figure 1 was much higher than those emitted to the left. However, in the case of Cavity #3, the intensity of the electrons emitted to the left in Figure 1 was much higher than those emitted to the right. Therefore, in this study, the field emission electron currents were measured in only the higher intensity directions (to the left in Cavity #3 and to the right in Cavity #4 in Figure 1).

The photon dose rates around the main superconducting cavities in the compact ERL room were measured using ThermoLuminescence Dosimeters (TLDs). This method is described in detail in Section 2.2. Furthermore, the photon dose rates on the roof of the compact ERL room were measured using survey meters. This method is described in Section 2.3.

The measured photon dose rates were compared with photon dose rates calculated by MARS15 [4] and converted into field emission electron current. The details of the MARS15 calculation and the method of converting a photon dose rate to a field emission electron current are described in Sections 3 and 4, respectively.

2.2 Measurement of photon dose rates around Cavities #3 and #4 using TLDs

2.2.1 Measurement procedures

TLDs (Panasonic, UD-813PQ4) were used to measure of the photon dose rates around the cavities. First, ten TLDs were installed around Cavity #4 on the beam height plane. The locations of the installed TLDs are shown in Figure 2a. To measure the photon dose rates from Cavity #4, 14.6 MV was applied to Cavity #4 for 22.49 min. (duration over 14.1 MV). After the operation, the TLDs were removed from the compact ERL room.

On a different day, 16 TLDs were installed on the beam height plane around Cavity #3 (exception: #11, #12, and #13 were +63 cm above the beam height). The locations of the installed TLDs are shown in Figure 2b. To measure the photon dose rates from Cavity #3, 13.5 MV of voltage was applied to Cavity #3 for 10.67 min. (duration over 13.0 MV). After the operation, the TLDs were removed from the compact ERL room.

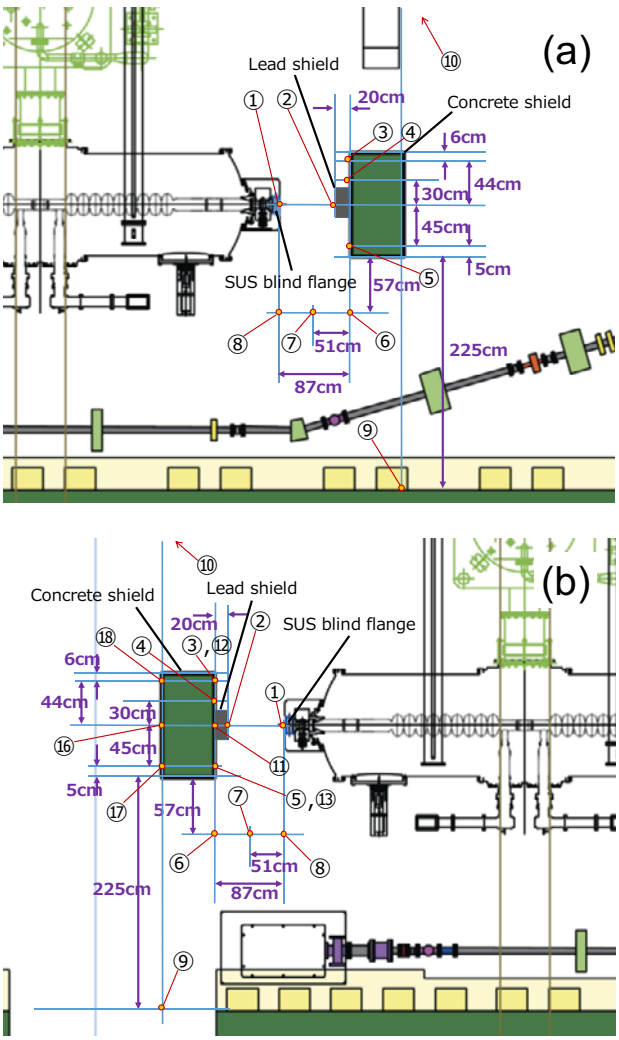

Fig. 2 a. Locations of the TLDs (#1 to #10) installed around Cavity #4 in the compact ERL room. **b.** Locations of the TLDs (#1 to #18, no #14 and #15) installed around Cavity #3 in the compact ERL room.

The photon dose could be read from each exposed TLD. Photon dose rates were obtained from the measured photon doses and the duration of applied voltage.

2.2.2 Measurement results

The measured photon dose rates around Cavities #4 and #3 are shown in Figures 3a and 3b, respectively. The photon dose rates were distributed from 0.011 to 382 Sv/h, depending on the location of the installed TLD. Though the voltage applied to Cavity #3 (13.5 MV) was lower than that applied to Cavity #4 (14.6 MV), the photon dose rate of Cavity #3 was much higher than Cavity #4. The field emission electron currents from Cavity #3 were found to be much higher than those of Cavity #4.

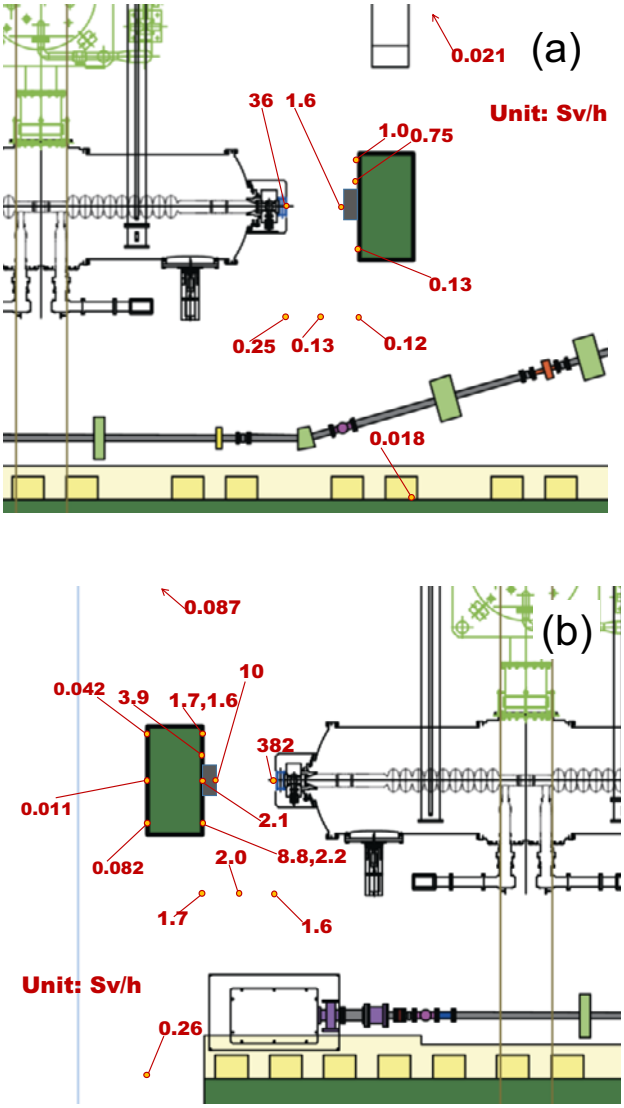

Fig. 3 a. Measured photon dose rates (Sv/h) from Cavity #4. **b.** Measured photon dose rates (Sv/h) from Cavity #3.

2.3 Photon dose rate measurement on the roof of the compact ERL room using survey meters

2.3.1 Measurement procedures

The photon dose rates on the roof of the compact ERL room during application of voltage to each cavity were measured using a NaI (Tl) scintillation survey meter (Aloka, Model: TCS-161) and an ionization chamber type survey meter (Aloka, Model: ICS-311). The shield structure of the compact ERL room is shown in Figure 4. The roof of the compact ERL room is concrete (thickness: 1 m, density: 2.32-2.36 g/cm^3). Field emission electrons travel along the beamline and hit the SUS blind flange at the red point in Figure 4. The distance between the ceiling of the room and beamline height is 2.8 m. The applied voltage was increased up to 13.5 MV for Cavity #3 and 15.5 MV for Cavity #4.

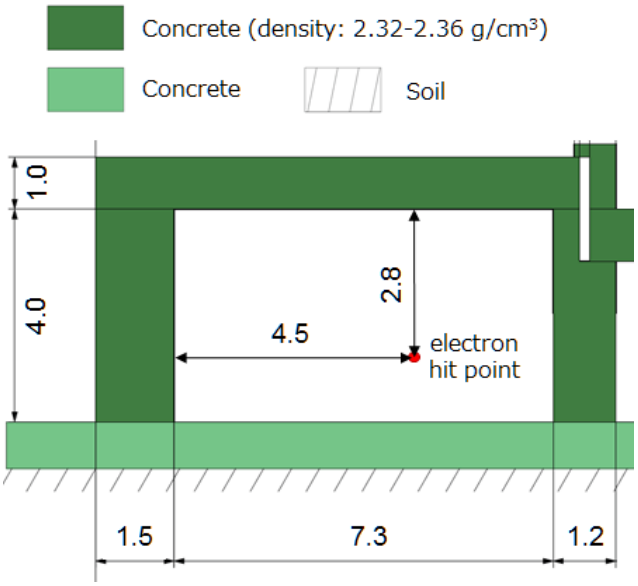

Fig. 4. Longitudinal-sectional view of the compact ERL room perpendicular to the flight direction of the field emission electron and including the electron hit point.

2.3.2 Measurement results

The maximum photon dose rate on the roof of the compact ERL room occurs just above the additional 50-cm-thick concrete shield. The photon dose rates obtained by the NaI (Tl) scintillation survey meter were comparable with those obtained by the ionization chamber type survey meter. The maximum photon dose rates measured by the NaI (Tl) scintillation survey meter are plotted as a function of applied voltage in Figure 5.

The field emission electron currents were found to increase steeply with applied voltage. Field emission from Cavity #3 began to increasing at an applied voltage ~2.5 MV lower voltage than for Cavity #4.

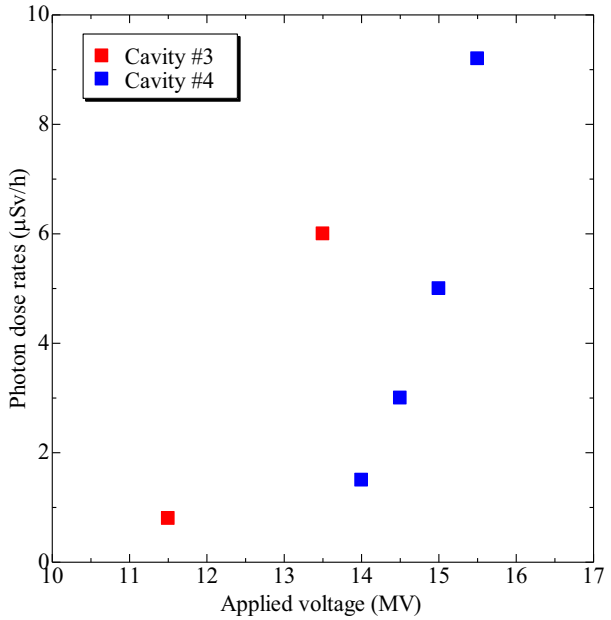

Fig. 5. Maximum photon dose rates measured on the roof of compact ERL room as a function of voltage applied to Cavities #3 and #4.

3 Calculation by MARS15

3.1. Calculation of photon dose rates by monochromatic energy electron

The photon dose rates (mSv/h) per μA of electron current were calculated using MARS15 for comparison with the measured dose rates in order to estimate field emission electron currents. In the MARS15 calculation, a SUS blind flange was bombarded with electrons at energies of 2.5, 5.0, 7.5, 10.0, 12.5, 15.0, 17.5, and 20.0 MeV. The density of the concrete roof was input as 2.34 g/cm^3. Then, the photon dose rates for each incident electron energy were obtained at the measurement locations.

As an example, a distribution of the calculated photon dose rates induced by 15.0 MeV electrons at 0.5 μA on the horizontal plane at incidence height is shown in Figure 6. In this calculation, the incident electrons struck the SUS blind flange perpendicular to its plane and at its center, although it has been observed that flight direction of the field emission electrons deviated a little from the center [6]. The strong photon dose rate was estimated to be in the forward direction.

Another example of a distribution of the calculated photon dose rates on the roof of the compact ERL room is shown in Figure 7. Here, energy and current of the incident electrons were also 15 MeV and 0.5 μA, respectively. As observed by the measurement, the maximum photon dose rate on the roof of the compact ERL room occurs just above the additional 50-cm-thick concrete shield.

The photon dose rates per μA electron current at the measurement locations calculated by MARS15 are plotted as a function of incident electron energy in Figure 8. The lines were obtained by least-square fits of a function to the plotted values. The photon dose rates increased with increasing incident electron energy.

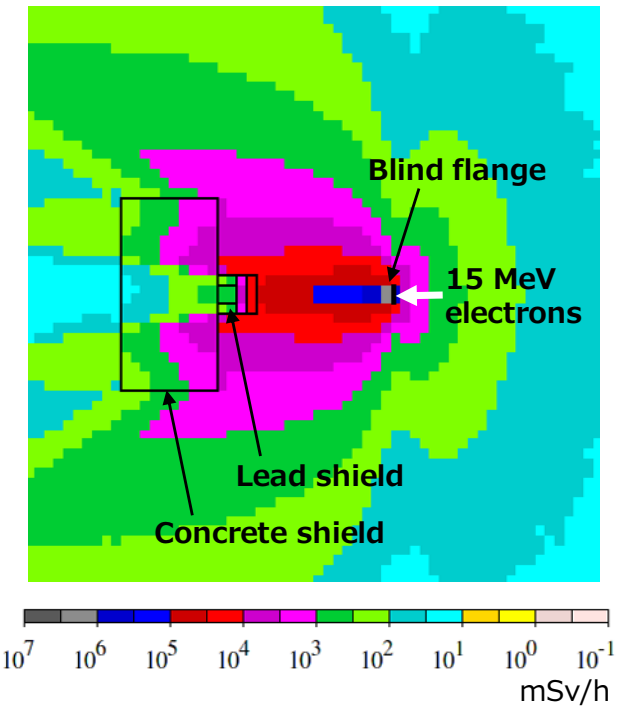

Fig. 6 Distribution of calculated photon dose rates induced by 15 MeV electrons at 0.5 μA on a horizontal plane at incidence height. The photon dose rate distribution was calculated by MARS15.

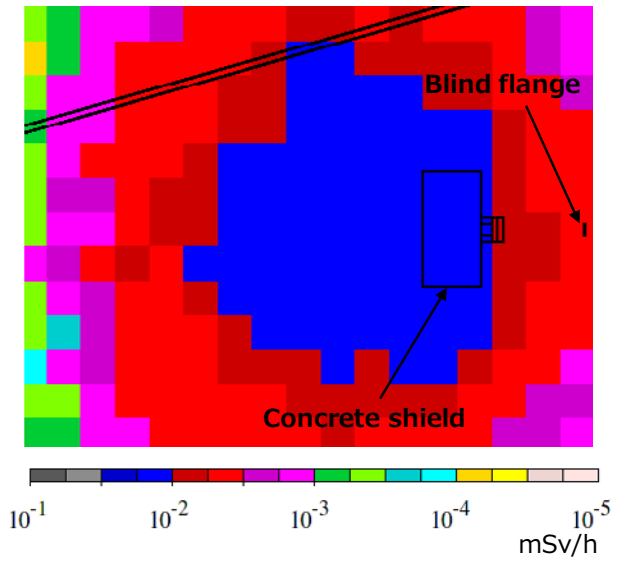

Fig. 7 Distribution of calculated photon dose rates induced by 15 MeV electrons at 0.5 μA on the roof of the compact ERL room. The photon dose rate distribution was calculated by MARS15.

3.2 Calculation of photon dose rates corresponding to the measured dose rates

The energies of the field emission electrons from the main superconducting cavities depend on the location at

which the electrons are generated [3]. Here, a uniform energy spectrum model can be applied to the field emission electrons to calculate the photon dose rate. Because the dose rates in Figure 8 were obtained by monochromatic energy electron, the calculated dose rate corresponding to the measured dose rate was obtained from the integral value of dose rate for monochromatic energy in Figure 8 from zero to a maximum energy. The field emission electron current was estimated by comparing the measured and calculated photon dose rates.

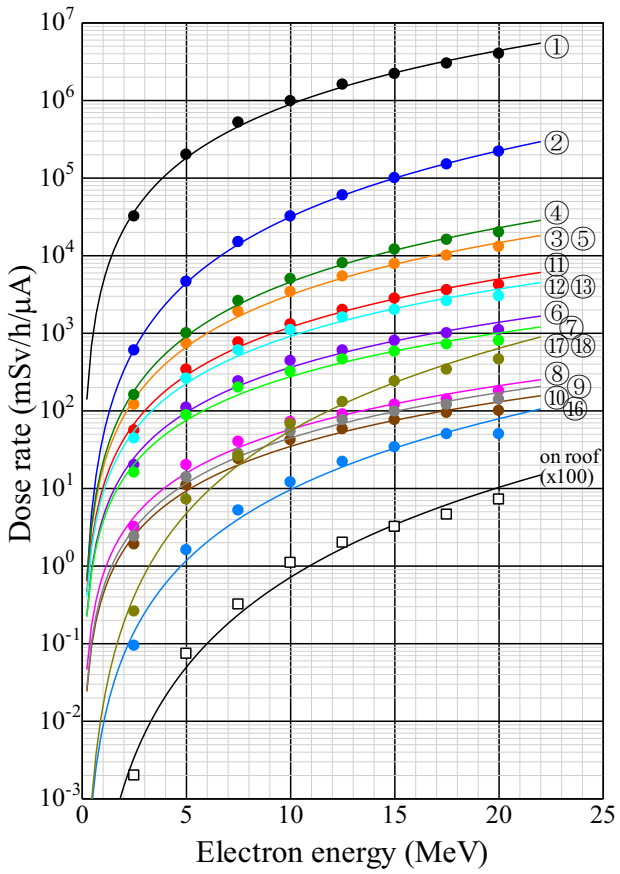

Fig. 8. Incident electron energy dependences of photon dose rates per μA electron current at the measurement locations calculated by MARS15. Numbers in circles correspond to the measurement locations shown in Figures 2a and 2b.

4 Field emission electron currents

4.1 Estimation from the photon dose rates measured around Cavities #3 and #4

The electron energy spectra were assumed to be distributed uniformly up to 12 MeV for Cavity #4 and up to 13 MeV for Cavity #3 at the SUS blind flange. Field emission electron currents arriving at the SUS blind flange from Cavities #3 and #4 were estimated by comparing the measured photon dose rate with the calculated photon dose rate. In Figure 9a and 9b, the field emission electron currents arriving at the SUS blind flange from Cavities #4 and #3, respectively, are indicated. These currents were estimated from photon dose rates for each location. The estimated field emission electron currents at locations #1, #2, and #8 were lower than others. This is due to the fact that the field emission trajectories are anisotropic, that was observed previously in [6]. The estimation at sharp and large angle directions is susceptible to the anisotropic trajectory. The estimated field emission electron currents agreed sufficiently for order estimation, except for the values at locations #1, #2, and #8 in Figures 2a and 2b.

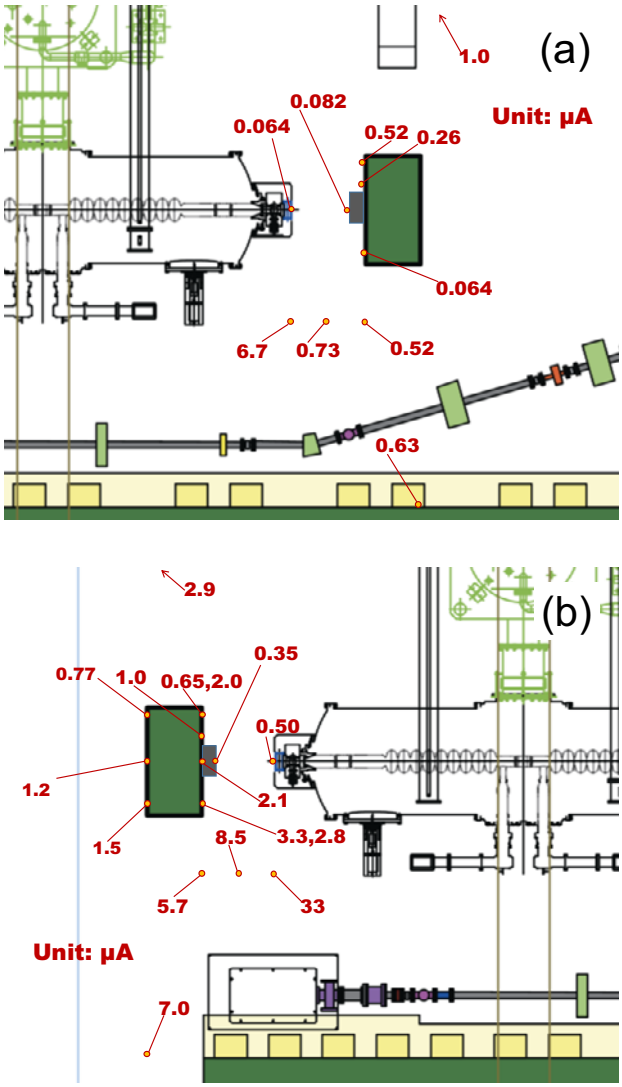

Fig. 9 a. Field emission electron currents (in units of μA) arriving at the SUS blind flange from Cavity #4. **b.** Field emission electron currents (in units of μA) arriving at the SUS blind flange from Cavity #3. The field emission electron currents were estimated from photon dose rates for respective locations.

The field emission electron current from Cavity #4 at 14.6 MV was estimated to be 0.53 ±0.30 μA. The field emission electron current from Cavity #3 at 13.5 MV was estimated to be 3.0 ±2.5 μA. These values were obtained as averages of individual estimated field emission electron currents (values at the locations #1, #2, and #8 in Figures 2a and 2b were omitted).

4.2 Estimation from the photon dose rates measured on the roof of the compact ERL room

The field emission electron currents arriving at the SUS blind flange from Cavities #3 and #4, estimated from the photon dose rates on the roof of the compact ERL room at various applied voltages, are plotted as a function of applied voltage in Figure 10. Here, we assumed that the electron spectra were distributed uniformly for energies up to 11 MeV (for 11.5 MV), 13 MeV (for 13.5, 14.0, and 14.5 MV), and 14 MeV (for 15.0 and 15.5 MV).

In the case of Cavity #3, the field emission electron current of 1.2 μA at 13.5 MV is consistent with 3.0 ±2.5 μA from the photon dose rates measured around Cavity #3 in Section 4.1. In the case of Cavity #4, the field emission electron current of 0.6 μA at 14.5 MV also agreed with 0.53 ±0.30 μA obtained previously in Section 4.1. Therefore, the photon dose rate on the roof is a good indicator of the field emission electron current. Field emission electron current increased exponentially as a function of applied voltage. Then, field emission electron current exceeding 1 μA was observed at 13.5 MV for Cavity #3 and at 15.5 MV for Cavity #4.

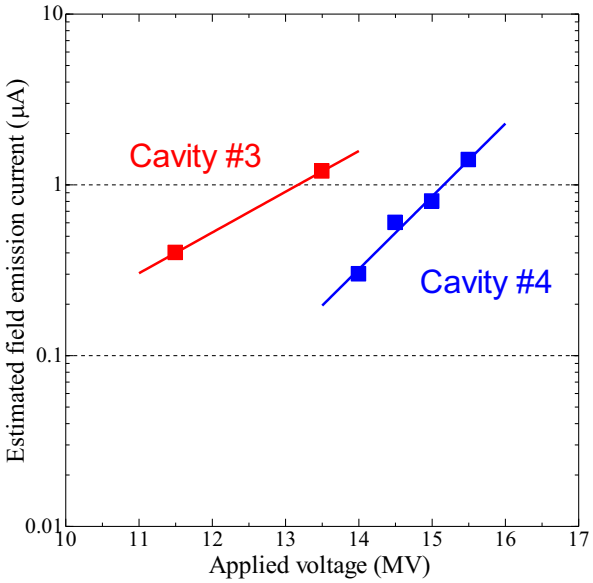

Fig. 10. Estimated field emission electron current arriving at the SUS blind flange fom Cavity #3 and Cavity #4 as a function of applied voltage. The values were estimated from the photon dose rates on the roof of the compact ERL room.

5 Conclusions

The field emission electron currents from the main superconducting cavities of compact ERL at KEK were estimated indirectly from photon dose rates measured around the cavities and on the roof of the compact ERL room. The field emission electron currents increased steeply with applied voltage. The field emission electron currents corresponding to the applied voltages were different between Cavities #3 and #4. The field emission electron current exceeding 1 μA was observed at 13.5 MV for Cavity #3 and at 15.5 MV for Cavity #4. In order to suppress the field emission electron current to sufficiently low level, 8.58 MV was applied to both Cavities #3 and #4 for the first recirculating loop operation in 2014.

References

1. T. Obina, M. Adachi, S. Adachi, T. Akagi, M. Akemoto, D. Arakawa, S. Araki, S. Asaoka, M. Egi, K. Enami, K. Endo, S. Fukuda, T. Furuya, K. Haga, K. Hara, K. Harada, T. Honda, Y. Honda, H. Honma, T. Honma, K. Hosoyama, K. Hozumi, A. Ishii, X. Jin, E. Kako, Y. Kamiya, H. Katagiri, H. Kawata, Y. Kobayashi, Y. Kojima, Y. Kondou, T. Konomi, A. Kosuge, T. Kume, T. Matsumoto, H. Matsumura, H. Matsushita, S. Michizono, T. Miura, T. Miyajima, H. Miyauchi, S. Nagahashi, H. Nakai, H. Nakajima, N. Nakamura, K. Nakanishi, K. Nakao, K. Nigorikawa, T. Nogami, S. Noguchi, S. Nozawa, T. Ozaki, F. Qiu, H. Sagehashi, H. Sakai, S. Sakanaka, S. Sasaki, K. Satoh, Y. Seimiya, T. Shidara, M. Shimada, K. Shinoe, T. Shioya, T. Shishido, M. Tadano, T. Tahara, T. Takahashi, R. Takai, H. Takaki, T. Takenaka, O. Tanaka, Y. Tanimoto, N. Terunuma, M. Tobiyama, K. Tsuchiya, T. Uchiyama, A. Ueda, K. Umemori, J. Urakawa, K. Watanabe, M. Yamamoto, N. Yamamoto, Y. Yamamoto, Y. Yano, M. Yoshida, R. Hajima, M. Mori, R. Nagai, N. Nishimori, M. Sawamura, T. Shizuma, M. Kuriki, *Recent developments and operational status of the compact ERL at KEK*, (Proceedings of IPAC2016, Busan, Korea, May 8-13, 2016)
2. H. Sakai, K. Enami, T. Furuya, M. Satoh, K. Shinoe, K. Umemori, M. Sawamura, E. Cenni, *High power CW tests of cERL main-linac cryomodule* (Proceedings of SRF2013, Paris, France, 2013).
3. E. Cenni, T. Furuya, H. Sakai, K. Umemori, K. Shinoe, M. Satoh, M. Sawamura, *Field emission simulation for KEK-ERL 9-cell superconducting cavity* (Proceedings of IPAC2012, New Orleans, USA, 2012)
4. H. Matsumura Y. Kishimoto, T. Miura, K. Hozumi, K. Haga, S. Sakanaka, K. Nigorikawa, S. Nagahashi, T. Obina and N. Nakamura, KEK-Internal **2015-6** (2015)
5. N. V. Mokhov, S. I. Striganov, *MARS15 overview*, (Proceedings of Hadronic Shower Simulation Workshop Fermilab September 2006), AIP Conf. Proc. **896**, 50 (2007)
6. E. Cenni, K. Enami, T. Furuya, H. Sakai, M. Satoh, K. Shinoe, K. Umemori, *Field emission measure during cERL main LINAC cryomodule high power test in KEK* (Proceedings of SRF2013, Paris, France, 2013)